LBL-23936
Preprint

Lawrence Berkeley Laboratory

UNIVERSITY OF CALIFORNIA

Materials & Chemical Sciences Division

NOV 10 1987
LIBRARY AND
DOCUMENTS SECTION

Submitted to the Journal of Electron
Spectroscopy and Related Phenomena

High Resolution UV Photoelectron Spectroscopy of CO_2^+, COS^+ and CS_2^+ Using Supersonic Molecular Beams

L. Wang, J.E. Reutt,
Y.T. Lee, and D.A. Shirley

September 1987

TWO-WEEK LOAN COPY
This is a Library Circulating Copy
which may be borrowed for two weeks.

Prepared for the U.S. Department of Energy under Contract DE-AC03-76SF00098

LBL-23936 c.2

DISCLAIMER

This document was prepared as an account of work sponsored by the United States Government. While this document is believed to contain correct information, neither the United States Government nor any agency thereof, nor the Regents of the University of California, nor any of their employees, makes any warranty, express or implied, or assumes any legal responsibility for the accuracy, completeness, or usefulness of any information, apparatus, product, or process disclosed, or represents that its use would not infringe privately owned rights. Reference herein to any specific commercial product, process, or service by its trade name, trademark, manufacturer, or otherwise, does not necessarily constitute or imply its endorsement, recommendation, or favoring by the United States Government or any agency thereof, or the Regents of the University of California. The views and opinions of authors expressed herein do not necessarily state or reflect those of the United States Government or any agency thereof or the Regents of the University of California.

LBL-23936

HIGH RESOLUTION UV PHOTOELECTRON SPECTROSCOPY OF CO_2^+, COS^+, AND CS_2^+ USING SUPERSONIC MOLECULAR BEAMS

Laisheng Wang, J.E. Reutt*

Y.T. Lee, and D.A. Shirley

Materials and Chemical Sciences Division

Lawrence Berkeley Laboratory

and Department of Chemistry

University of California

Berkeley, California 94720

*Present address: AT&T Bell Laboratories

Room MH 1C-333, 600 Mountain Avenue

Murray Hill, NJ 07974

ABSTRACT

Very high resolution HeI (584Å) photoelectron spectra of CO_2^+, COS^+, and CS_2^+ are presented. The spectra were obtained by using supersonic molecular beams to eliminate the rotational and Doppler broadenings. The spin-orbit split components in the Π bands are all explicitly resolved. The removal of the inelastic scattering peaks, due to the use of molecular beams, allowed new features to be observed in the $\tilde{B}$ and $\tilde{C}$ bands of CS_2^+, and new spectroscopic constants were derived.

INTRODUCTION

Since its birth in the 60s [1-6], molecular photoelectron spectroscopy (PES) grew quickly to its maturity in the next decade [7]. It has contributed profoundly to our understanding of the electronic properties of atoms and molecules [8]. A major development in the field, after its initial success, was the significant improvement of the resolution and data acquisition rate. Much of this progress is credited to Dr. Kai Siegbahn and his group at Uppsala, for their introduction and application of the multichannel detection technique to UV-valence photoelectron spectroscopy [9-13]. As a result of the improved resolution, such spectroscopic details as vibrational fine structure, vibronic interaction (Renner-Teller effect and John-Teller effect), and vibrational-vibrational interaction (Fermi resonance), etc., become possible for study in small polyatomic molecules [14-19].

Due to the room temperature sampling of the target molecules, photoelectron spectra, so obtained, often didn't achieve the ultimate instrumental resolution, because of the rotational broadening and the Doppler broadening. Hence, it was apparent that further progress in the field relied on the marriage of the photoelectron spectroscopy and the molecular beam technique [20-22]. By sampling the photoelectrons perpendicular to the molecular beam, one can completely eliminate the Doppler broadening. And the rotational cooling associated with the supersonic expansion can substantially reduce the rotational broadening. In addition, molecular beams provide a clean environment to perform experiments by means of differential pumping. Consequently, inelastic

scattering of photoelectrons by background molecules, and surface contamination of critical elements in the spectrometer are diminished, and very high resolution spectra can be obtained [23-27]. In this paper, we use the molecules CO_2, COS, and CS_2 to demonstrate the capabilities of the technique. The above-mentioned advantages are fully realized: the spin-orbit split components in all the Π bands are completely resolved, and the inelastic scattering features in the $\tilde{X}$ and $\tilde{C}$ bands of CO_2^+ and CS_2^+ [19,28,29] are completely removed.

The photoelectron spectra of CO_2^+, COS^+, and CS_2^+ have been extensively studied since the beginning of the field [30-34] and are still under study [19,28,29,35-43]. The isoelectronic structures of the three molecules are ideal for observing any systematic changes. Observations of the Renner-Teller effect and Fermi resonances have also motivated several investigations [36,37,40]. High resolution HeI photoelectron spectra are available for the three molecules [19,29,39]. Due to the still inferior resolution in the room temperature spectra, however, none of the previous HeI work was able to completely resolve the spin-orbit split components of the $\tilde{A}$ bands of CO_2^+ and COS^+. Some vibrational assignments have also been controversial [34,39]. Pressure dependent studies have been conducted for CO_2^+ and CS_2^+, and the inelastic scattering features in the $\tilde{X}$ and $\tilde{C}$ bands have been confirmed [19,29]. However, the drastic reduction of the ν_3 value in the $\tilde{X}$ state of CO_2^+ remains largely unresolved [34], as does the broadening of the $\tilde{A}$ band of CS_2^+ [29]. The current study, with superior resolution and rotational cooling, was designed to provide high quality HeI PE spectra, validate the earlier work, and make further analyses.

Experimental parameters are described in the next section. In the following section, results are presented and discussed for the three molecular ions CO_2^+, COS^+, and CS_2^+ together, organized under four subsections covering the $\tilde{X}$, $\tilde{A}$, $\tilde{B}$, and $\tilde{C}$ states in turn. A brief summary appears at the end.

EXPERIMENTAL

The molecular beam photoelectron spectrometer used for this study has been described in detail elsewhere [22]. Only a brief description will be given here. A schematic top view of the apparatus is shown in Fig. 1. The main feature is the coupling of the molecular beam source to the photoelectron spectrometer, which has a hemispherical energy analyzer and a multichannel detector. The molecular beams, which were expanded out through a small nozzle (70 μm for CO_2, 200 μm for COS and CS_2) and skimmed by a conical skimmer (0.66 mm diam. for CO_2, 0.91 mm diam. for COS and CS_2), propagated horizontally into the interaction region where it crossed perpendicularly with the photon beam from a helium discharge lamp. The lamp, which is not shown in Fig. 1, sat on the top of the chamber. The photoelectrons were detected at 90° with respect to both the molecular beams and the photon beam.

All samples were of commercial origin. Pure CO_2 was expanded at a stagnation presure of 900 torr, and COS at 310 torr. CS_2 was run by passing about 250 torr He through the ice-trapped CS_2 (55 torr CS_2 vapor). A bigger nozzle was used for COS and CS_2 to prevent clustering during the supersonic expansion. The analyzer pass energy was set at

1 eV, which determined the maximum scan width to be 2.5 eV. Therefore, the CO_2^+ and COS^+ spectra were taken by three scans sequentially, and CS_2^+ by four. Each scan was kept within two hours, and an Ar photoelectron spectrum was taken following each scan for calibration. The energy scale shift was within ± 2 meV for each scan. The resolution (FWHM) as measured for the Ar^+ $^2P_{3/2}$ was 12 meV during the CO_2^+ scans, and 13 meV during the COS^+ and CS_2^+ scans.

RESULTS AND DISCUSSION

The HeI photoelectron spectra of CO_2^+, COS^+, and CS_2^+ are shown in Fig. 2. All spectra are plotted to the full scale of the $\tilde{X}$ bands. Each spectrum contains four bands, resulting from the ionization of the four outermost molecular orbitals (MOs) of each molecule. Since the three molecules are isoelectronic, they have similar valence MOs and similar valence photoelectron spectra, with the ionization potentials (IPs) decreasing from CO_2 to CS_2. The $\tilde{A}$ and $\tilde{B}$ bands are partially overlapped in CO_2^+ and COS^+, but fully separated in CS_2^+. In addition, there are two extra, weak bands in CS_2^+, which have been previously identified as two CI satellite bands [29]. The assignment and detailed analysis of each band and the discussions are given below. The derived ionization potentials and spectroscopic constants from this experiment are tabulated in Table 1 and Table 2 respectively.

The $\tilde{X}$ bands ($^2\Pi_g$ for CO_2^+ and CS_2^+, $^2\Pi$ for COS^+)

The $\tilde{X}$ band spectra are displayed separately in Fig. 3. These bands correspond to the ionization of an essentially non-bonding electron localized on an O or S atom. Hence, very little vibrational excitation is observed. In CO_2^+ and CS_2^+, the only vibronically allowed transition is to the ν_1 mode. A combination of ν_1 and ν_3 modes is observed in COS^+, since both are equally allowed. The spin-orbit interaction is very strong in the $\tilde{X}$ bands, so each vibrational peak is clearly a doublet. The IPs and the assignment are summarized in Tables 3-5.

The Renner-Teller effect has been discussed for CO_2^+ previously [19,36,41], and will not be belabored here. This effect is much weaker in COS^+ and CS_2^+.

In CO_2^+, the features above 14.05 eV were resolved in only two previous accounts, by Reineck et al [19] with HeI excitation and by Baer and Guyon [43] with threshold PES (TPES) using synchrotron radiation. The observation of the (0 0 2) peak provides us with a ν_3 value of 1470 cm^{-1}, which agrees with the previous measurements [19,43]. This ν_3 value is much lower than that of CO_2 (2349 cm^{-1} [44]). Brundle and Turner ascribed this reduction to the bent geometry of CO_2^+ in their early study [34], based on a then-available Franck-Condon analysis [45]. However, Reineck et al [19] recently attributed it to a strong vibrational coupling effect. In a recent ab initio calculation, Praet et al [46] suggested that CO_2^+ was bent in the ground state, with an equilibrium angle of 172°. In a later calculation, Grimm and Larsson [47] concluded that the four lowest doublet states of CO_2^+ were linear. Since Grimm and Larsson emphasized on the $\tilde{A}$, $\tilde{B}$, and $\tilde{C}$ states only, we still prefer the result from Praet et al for the $\tilde{X}$ state. Although the

equilibrium angle of 172° is not much different from the linear geometry, it would significantly change the force field of the ν_3 vibration. On this ground, we interpret the dramatic change of ν_3 as a result of the bent CO_2^+ structure.

The assignment of the $\tilde{X}$ band of COS^+ agrees with previous studies [39]. For CS_2^+, the inelastic scattering features encountered by Reineck et al [29] completely disappear in the present spectra, enabling us to observe $1\nu_3$. The ν_3 value we obtain is 1200 cm^{-1}, given in Table 2. This value agrees better with that obtained by optical spectroscopy [48] than those previously reported [29,38].

The $\tilde{A}$ bands ($^2\Pi_u$ for CO_2^+ and CS_2^+, $^2\Pi$ for COS^+)

The $\tilde{A}$ bands are shown in Fig. 4. A broad vibrational band is observed in each case, following the photoionization from the Π bonding orbitals. The spin-orbit splittings are much smaller than those in the ground states, and the spin-orbit split components in CO_2^+ and COS^+ have not been explicitly resolved previously following HeI excitation. With the aid of rotational cooling, we were able to resolve the two components of each peak, as shown in Fig. 4. Derived spin-orbit coupling constants are listed in Table 2. They are in good agreement with TPES measurements [36,37], and particularly with those obtained by optical spectroscopy [49]. The peak assignments and IPs are summarized in Tables 6-8.

The stretching vibrations are the predominant excitations evident in all three molecular ion spectra. For CO_2^+, there is also a weak structure below each main stretching peak. These features have been

assigned in different ways before, either as $2\nu_2$ [41] or as a sequential hot band transition [19]. The features below the (0 0 0) peak are certainly due to hot band transitions. We prefer to assign the rest as $2\nu_2$, as shown in Fig. 4, because the $2\nu_2$ transitions are allowed on the symmetry grounds. Baer and Guyon [43] clearly observed the $2\nu_2$ transitions as well as the hot band transitions.

As in the $\tilde{X}$ band, the $\tilde{A}$ band of COS^+ also contains a series of ν_1 and ν_3 stretching peaks. A previous high resolution study assigned only two quanta of ν_3 [39], but the ν_3 excitation should be at least as extensive as ν_1, since both are allowed. Our assignment is shown in Fig. 4. There may well be additional ν_3 series which overlap with the $\tilde{B}$ band. The ν_2 mode is also weakly excited, as indicated in Table 7.

For CS_2^+, the origin of the first sharp peak had long been uncertain [38]. This peak is due to the HeI β line spectrum of the $\tilde{B}$ state, as assigned by Reineck et al [29]. The spectrum at higher IP is significantly broadened even with the rotational cooling in this experiment. The lowest energy dissociation channel is well above the $\tilde{A}$ band (14.81 eV [50]). Thus neither life-time nor rotational broadening is responsible for this broadening, which has been attributed to the superposition of $2\nu_2$ [29]. Indeed the $2\nu_2$ peaks have been observed to be very close to the $1\nu_1$ energies in a previous TPES study by Frey et al [37]. The Fermi resonance between $1\nu_1$ and $2\nu_2$ would further broaden the ν_1 progression [37].

The $\tilde{B}$ bands ($^2\Sigma_u^+$ for CO_2^+ and CS_2^+, $^2\Sigma^+$ for COS^+)

The $\tilde{B}$ bands are shown in Fig. 5, and the derived IPs and assignments are listed in Tables 9-11. Overlap with the $\tilde{A}$ bands in CO_2^+ and COS^+ makes these assignments much more difficult. Wannberg et al [42] obtained a high resolution spectrum of the $\tilde{B}$ band of CO_2^+, using polarized HeI radiation, and made a complete assignment in agreement with the assignment in Table 9. The $\tilde{B}$ band of COS^+ can be only partially assigned, as shown in Fig. 5, because of overlap with the $\tilde{A}$ band.

The $\tilde{B}$ band of CS_2^+ is fully separated from the $\tilde{A}$ band. A simple spectrum with very little vibrational excitation is observed. Strong inelastic scattering features were observed by Reibeck et al [29] in their high resolution study of CS_2^+. The complete disappearance of these features allows us to observe the (0 0 2) peak unambiguously, permitting a ν_3 value of 1320 cm^{-1} to be derived for the first time.

The $\tilde{C}$ bands ($^2\Sigma_g^+$ for CO_2^+ and CS_2^+, $^2\Sigma^+$ for COS^+)

These last bands are shown in Fig. 6. The IPs and assignments are listed in Tables 9-11, along with the $\tilde{B}$ bands.

There have been a lot of studies and some controversies concerning the $\tilde{C}$ band of CO_2^+ [19,28]. A study by Eland and Berkowitz [28] clearly showed a new peak at 19.68 eV, which they assigned as $1\nu_3$. Later this peak was proved by Reineck et al [19] to be an inelastic scattering peak. This peak distinctly disappeared in the present spectrum. The peak at 19.75 eV has also been subject to dispute [19,41,43,47]. Reineck et al [19] assigned it as (1 0 1), based on asymmetry parameter measurements [51]. Strong vibronic interaction between the $\tilde{C}$ and $\tilde{B}$

states was invoked to explain the unusually high intensity of this forbidden transition. Grimm and Larsson [47] reassigned this peak as (0 0 1). The assignment of the peak as (1 0 1) was supported by the ^{13}C isotopic substitution experiment of Baer and Guyon [43]. We agree with this assignment and derive a ν_3 value of 1567 cm^{-1}, listed in Table 2. The doublet peak, assigned to (1 0 0) and (0 2 0) in Fig. 6, is a Fermi resonance, as interpreted by Reineck et al [19]. Our ν_1 value, shown in Table 2, was derived by taking this effect into account.

The assignment of the $\tilde{C}$ band of COS^+ is straightforward. It is primarily a combination of ν_1 and ν_3, with little ν_2. The assignment, shown in Fig. 6, agrees with previous studies [39,40]. The very low intensity of the (0 0 3) peak in the current spectrum was caused by the deteriorated analyzer transmission during the experiment.

Very strong inelastic scattering features were observed in the $\tilde{C}$ band of CS_2^+ by Reineck et al [29]. The complete elimination of these extrinsic peaks allowed us to resolve two new peaks at 16.4 eV and 16.44 eV. The peak at 16.44 eV can easily be assigned to (3 0 0). By analogy to the $\tilde{C}$ band of CO_2^+, we assign the peak at 16.4 eV to (1 0 1), which gives a ν_3 value of 1024 cm^{-1}, as shown in Fig. 2. The observation of (1 0 1) along with (0 1 0) signifies strong vibronic interaction in the $\tilde{C}$ state of CS_2^+, similar to the $\tilde{C}$ state of CO_2^+.

SUMMARY

By using molecular beams, very high effective resolution was achieved and inelastic scattering of photoeletrons was eliminated. We

not only resolved the spin-orbit components in all possible bands of the three molecular ions, but also observed new features in the $\tilde{B}$ and $\tilde{C}$ bands of CS_2^+. Many previous findings were confirmed, and new spectroscopic constants were derived. Strong vibronic interactions were observed in the $\tilde{X}$ and $\tilde{C}$ states of CO_2^+, and in the $\tilde{C}$ state of CS_2^+.

ACKNOWLEDGMENT

This work was supported by the Director, Office of Energy Research, Office of Basic Energy Sciences, Chemical Science Division of the U.S. Department of Energy under Contract No. DE-AC03-76SF00098.

REFERENCE

1. F.I. Vilesov, B.L. Kurbatov and A.N. Terenin, Sov. Phys. Dokl., 6 (1961) 490.
2. D.W. Turner and M.I. Al-Joboury, J. Chem. Phys., 37 (1962) 3007.
3. R.I. Schoen, J. Chem. Phys., 40 (1964) 1830.
4. D.C. Frost, C.A. McDowell and D.A. Vroom, Phys. Rev. Lett., 15 (1965) 612.
5. A.W. Potts, H.J. Lempka, D.G. Streets and W.C. Price, Phil. Trans. Roy. Soc. London A, 268 (1970) 59.
6. D.W. Turner, C. Baker, A.D. Baker and C.R. Brundle, Molecular Photoelecton Spectroscopy, Wiley-Interscience, London, 1970.
7. J.W. Rabalais, Principle of Ultraviolet Photoelectron Spectroscopy, John Wiley & Sons, New York, 1977.
8. J.H.D. Eland, Photoelectron Spectroscopy, Butterworths, London, 1984.
9. K. Siegbahn, D. Hammond, H. Fellner-Feldegg and E.F. Barnett, Science, 176 (1972) 245.
10. U. Gelius, E. Basilier, S. Svensson, T. Bergmark and K. Siegbahn, J. Electron Spectrosc. Relat. Phenom., 2 (1974) 405.
11. L. Karlsson, L. Mattsson, R. Jadrny, R.G. Albridge, S. Pinchas, T. Bergmark and K. Siegbahn, J. Chem. Phys., 62 (1975) 4745.
12. L. Karlsson, L. Mattsson, R. Jadrny, Bergmark and K. Siegbahn, Phys. Scr., 13 (1976) 229.
13. L. Karlsson, L. Mattsson, R. Jadrny, Bergmark and K. Siegbahn, Phys. Scr., 14 (1976) 230.

14. J.W. Rabalais, L. Karlsson, L.O. Werme, T. Bergmark and K.Siegbahn, J. Chem. Phys., 58 (1973) 3370.

15. R. Jadrny, L. Karlsson, L. Mattsson and K. Siegbahn, Phys. Scr., 16 (1977) 235.

16. L. Karlsson, R. Jadrny, L.Mattsson, F.T. Chau and K. Siegbahn, Phys. Scr., 16 (1977) 225.

17. R. Jadrny, L. Karlsson, L. Mattsson and K. Siegbahn, Chem. Phys. Lett., 49 (1977) 203.

18. R. Maripuu, I. Reineck, H. Agren, N. Wu, J. Rong, H. Veenhuizen, S. H. Al-Shamma, L. Karlsson and K. Siegbahn, Mol. Phys., 48 (1983) 1255.

19. I. Reineck, C. Nohre, R. Maripuu, P. Lodin, S.H. Al-Shamma, H. Veenhuizen, L. Karlsson and K. Siegbahn, Chem. Phys., 78 (1983) 311.

20. J.H.D. Eland, J. Phys. E : Sci. Instrum., 11 (1978) 969.

21. P.M. Dehmer and J.L. Dehmer, J. Chem. Phys., 70 (1979) 4574.

22. J.E. Pollard, D.J. Trevor, Y.T. Lee and D.A. Shirley, Rev. Sci. Instrum., 52 (1981) 1837.

23. J.E. Pollard, D.J. Trevor, J.E. Reutt, Y.T. Lee and D.A. Shirley, J. Chem. Phys., 77 (1982) 34.

24. J.E. Reutt, L.S. Wang, J.E. Pollard, D.J. Trevor, Y.T. Lee and D.A. Shirley, J. Chem. Phys., 84 (1986) 3022.

25. J.E.Reutt, L.S. Wang, Y.T. Lee and D.A. Shirley, J. Chem. Phys., 85 (1986) 6928.

26. L.S. Wang, J.E. Pollard, Y.T. Lee and D.A. Shirley, J. Chem. Phys. 86 (1987) 3216.

27. L.S. Wang, Y.T. Lee and D.A. Shirley, J. Chem. Phys., 87 (1987) 2489.

28. J.H.D. Eland and J. Berkowitz, J. Chem. Phys., 67 (1977) 2782.

29. I. Reineck, B. Wannberg, H. Veenhuizen, C. Nohre, R. Maripuu, K.E. Norell, L. Mattsson, L. Karlsson and K. Siegbahn, J. Electron Spectrosc. Relat. Phenom., 34 (1984) 235.

30. M.I. Al-Joboury, D.P. May, and D.W. Turner, J. Chem. Soc., (1965) 6350.

31. D.W. Turner and D.P. May, J. Chem. Phys., 46 (1967) 1156.

32. J.H.D. Eland and C.J. Danby, Int. J. Mass Spectom. Ion Phys., 1 (1968) 111.

33. J.E. Collin and P. Natalis, Int. J. Mass Spectrom. Ion Phys., 1 (1968) 121.

34. C.R. Brundle and D.W. Turner, Int. J. Mass Spectrom. Ion Phys., 2 (1969) 195.

35. C.F. Batten, J.A. Taylor and G.G. Meisels, J. Chem. Phys., 65 (1976) 3316.

36. R. Frey, B. Gotchev, O.F. Kalman, W.B. Peatman, H. Pollak and E.W. Schlag, Chem. Phys., 21 (1977) 89.

37. R. Frey, B. Gotchev, W.B. Peatman, H. Pollak and E.W. Schlag, Int. J. Mass Spectrom. Ion Phys., 26 (1978) 137.

38. M.J. Hubin-Franskin, J. Delwiche, P. Natalis, G. Caprace and D. Roy, J. Electron Spectrosc. Relat. Phenom., 18 (1980) 295.

39. J. Delwiche, M.J. Hubin-Franskin, G. Caprace, P. Natalis and D. Roy, J. Electron Spectrosc. Relat. Phenom., 21 (1980) 205.

40. A.W. Potts and G.H. Fattahallah, J. Phys. B : At. Mol. Phys.,

13 (1980) 2545.

41. B. Kovac, J. Chem. Phys., 78 (1983) 1684.
42. B. Wannberg, H. Veennhuizen, L. Mattsson, K.E. Norell, L. Karlsson and K. Siegbahn, J. Phys. B : At. Mol. Phys., 17 (1984) L259.
43. T. Baer and P.M. Guyon, J. Chem. Phys., 85 (1986) 4765.
44. G. Herzberg, Molecular Spectra and Molecular Structure. III. Electronic Spectra and Electronic Structure of Polyatomic Molecules, Van Nostrand Reinhold Company, New York, 1966, P598.
45. V.A. Koryashkin, Dokl. Akad. Nank SSSR, 167 (1966) 1035.
46. M.T. Praet, J.C. Lorguet and G. Raseev, J. Chem. Phys., 77 (1982) 4611.
47. F.A. Grimm and M. Larsson, Phys. Scr., 29 (1984) 337.
48. W.J. Balfour, Can. J. Phys., 54 (1976) 1969.
49. D. Gauyacq, C. Larcherand and J. Rostas, Can. J. Phys., 57 (1979) 1634.
50. B. Brehm, J.H.D. Eland, R. Frey and A. Kustler, Int. J. Mass Spectroom. Ion Phys., 12 (1973) 213.
51. J. Kreile and A. Schweig, J. Electron Spectrosc. Relat. Phenom., 20 (1980) 191.

TABLE 1

ADIABATIC IONIZATION POTENTIALS (eV) OF CO_2, COS AND CS_2[a].

	$\tilde{X}\ ^2\Pi_g$	$\tilde{A}\ ^2\Pi_u$	$\tilde{B}\ ^2\Sigma_u^+$	$\tilde{C}\ ^2\Sigma_g^+$
CO_2	13.778[b]	17.314	18.077	19.394
COS	11.185	15.078	16.042	17.957
CS_2	10.080	12.698	14.477	16.190

a. The g and u symmetries do not apply for COS.

b. The uncertainties are ± 0.002 eV.

TABLE 2

VIBRATIONAL ENERGIES (cm^{-1}) AND SPIN-ORBIT SPLITTING CONSTANTS (A) (cm^{-1}) FOR CO_2^+, COS^+ AND CS_2^+.

		ν_1	ν_2	ν_3	A
CO_2^+	$\tilde{X}\ ^2\Pi_g$	1264(1)[a]		1470(1)[b]	158(4)[c]
	$\tilde{A}\ ^2\Pi_u$	1126(3)[a]	459(8)[d]		96(8)[c]
	$\tilde{B}\ ^2\Sigma_u^+$	1275(1)[a]	557(4)[a]	1840(5)[a]	
	$\tilde{C}\ ^2\Sigma_g^+$	1352(4)[a,e]	614(4)[a]	1567(4)	
COS^+	$\tilde{X}\ ^2\Pi$	706(2)[a]	476(16)[a]	2075(4)[a]	372(3)[c]
	$\tilde{A}\ ^2\Pi$	812(4)[a]	336(20)[d]	2036(6)[a]	113(6)[c]
	$\tilde{B}\ ^2\Sigma^+$	742(7)[a]	515(3)[a]	1850(8)[a]	
	$\tilde{C}\ ^2\Sigma^+$	926(5)[a]	454(5)[a]	2202(2)[a]	
CS_2^+	$\tilde{X}\ ^2\Pi_g$	660(2)[a]		1200(4)[b]	436(2)[c]
	$\tilde{A}\ ^2\Pi_u$	585(2)[a]			172(4)[c]
	$\tilde{B}\ ^2\Sigma_u^+$	633(2)[a]	351(5)[a]	1320(5)[b]	
	$\tilde{C}\ ^2\Sigma_g^+$	657(2)[a]	348(9)[a]	1024(6)	

a. Determined from the v = 1 peak.

b. $1/2(2\nu_3)$.

c. Determined from the (0 0 0) peak.

d. $1/2(2\nu_2)$.

e. Corrected for the Fermi resonance (see text).

TABLE 3

IONIZATION POTENTIALS AND VIBRATIONAL ASSIGNMENTS OF THE $\tilde{X}\ ^2\Pi_g$ PHOTOELECTRON BAND OF CO_2^+.

IP (eV)	Vibrational assignment	
	$\Omega = 3/2$	$\Omega = 1/2$
13.7579(3)[a]	2_1^1 (H.B.)	
13.7778(1)	0 0 0	
13.7973(1)		0 0 0
13.8381(3)	0 1 0	
13.8655(4)		0 1 0
13.8947(3)	0 2 0	
13.9169(10)		0 2 0
13.9344(1)	1 0 0	
13.9542(1)		1 0 0
13.9640(9)	0 0 1	
13.9959(8)	1 1 0	
14.0271(7)		1 1 0
14.0548(4)	1 2 0	
14.0886(1)	2 0 0	
14.1086(1)		2 0 0
14.1255(9)	2 1 0	
14.1423(1)	0 0 2	
14.1612(1)		0 0 2

14.2918(1)	1 0 2	
14.3120(1)		1 0 2
14.4407(7)	2 0 2	
14.4600(20)		2 0 2
14.4900(40)	0 0 4	

a. The absolute peak positions can only be determined within ± 0.002 eV. The relative peak positions for calculating vibrational energies may be determined more accurately. This is noted parenthetically.

TABLE 4

IONIZATION POTENTIALS AND VIBRATIONAL ASSIGNMENTS OF THE $\tilde{X}\ ^2\Pi$ PHOTOELECTRON BAND OF COS^+.

IP (eV)	Vibrational assignment	
	$\Omega = 3/2$	$\Omega = 1/2$
11.0797(6)[a]	1_1^0 (H.B.)	
11.1248(9)		1_1^1 (H.B.)
11.1853(1)	0 0 0	
11.2314(1)		0 0 0
11.2726(1)	1 0 0	
11.2900(20)		0 1 0
11.3191(1)		1 0 0
11.3320(20)	1 1 0	
11.3585(1)	2 0 0	
11.3760(20)		1 1 0
11.4048(1)		2 0 0
11.4426(1)	0 0 1	
11.4885(1)		0 0 1
11.5304(1)	1 0 1	
11.5447(20)		0 1 1
11.5766(1)		1 0 1
11.5920(20)	1 1 1	
11.6176(2)	2 0 1	

11.6312(20)		1 1 1
11.6626(2)		2 0 1
11.6942(2)	0 0 2	
11.7416(2)		0 0 2
11.7835(3)	1 0 2	
11.8284(3)		1 0 2
11.8730(15)	2 0 2	
11.9160(15)		2 0 2

a. See footnote a in TABLE 3.

TABLE 5

IONIZATION POTENTIALS AND VIBRATIONAL ASSIGNMENTS OF THE $\tilde{X}\ ^2\Pi_g$ PHOTOELECTRON BAND OF CS_2^+.

IP (eV)	Vibrational assignment	
	$\Omega = 3/2$	$\Omega = 1/2$
10.0807(1)[a]	0 0 0	
10.1347(1)		0 0 0
10.1625(2)	1 0 0	
	0 2 0	
10.2233(5)		1 0 0
		0 2 0
	2 0 0	
10.2829(3)		2 0 0
10.2894(9)		0 0 1
10.3780(3)	0 0 2	
10.4310(3)		0 0 2
10.4598(9)	1 0 2	
10.5221(11)		1 0 2
10.6885(23)	0 0 4	
10.7345(27)		0 0 4

a. See footnote a in TABLE 3.

TABLE 6

IONIZATION POTENTIALS AND VIBRATIONAL ASSIGNMENTS OF THE $\tilde{A}\ ^2\Pi_u$ PHOTOELECTRON BAND OF CO_2^+.

IP (eV)	Vibrational assignment	
	$\Omega = 3/2$	$\Omega = 1/2$
17.1603(9)[a]		1_1^0 (H.B.)
17.2888(10)	2_1^1	
17.3145(2)	0 0 0	
17.3264(2)		0 0 0
17.4295(9)	0 2 0	
17.4540(1)	1 0 0	
17.4659(1)		1 0 0
17.5665(9)	1 2 0	
17.5941(1)	2 0 0	
17.6058(1)		2 0 0
17.7068(8)	2 2 0	
17.7312(2)	3 0 0	
[illegible]		[illegible]

18.0182(2)		5 0 0
18.1123(20)	5 2 0	
18.1397(10)	6 0 0	
18.1519(10)		6 0 0
18.2530(30)	6 2 0	
18.2785(6)	7 0 0	
18.2927(7)		7 0 0
18.4137(10)	8 0 0	
18.4249(50)		8 0 0
18.5572(50)	9 0 0	
18.6872(10)	10 0 0	
18.8190(60)	11 0 0	

a. See footnote a in TABLE 3.

TABLE 7

IONIZATION POTENTIALS AND VIBRATIONAL ASSIGNMENTS OF THE $\tilde{A}\ ^2\Pi$ PHOTOELECTRON BAND OF COS^+.

IP (eV)	Vibrational assignment	
	$\Omega = 3/2$	$\Omega = 1/2$
14.9723(10)[a]	1_1^0 (H.B.)	
15.0550(15)	2_1^1 (H.B.)	
15.0775(3)	0 0 0	
15.0919(3)		0 0 0
15.1609(9)	0 2 0	
15.1782(2)	1 0 0	
15.1927(3)		1 0 0
15.2645(9)	1 2 0	
15.2784(3)	2 0 0	
15.2922(3)		2 0 0
15.3298(3)	0 0 1	
15.3441(2)		0 0 1
15.3701(10)	2 2 0	
15.3779(3)	3 0 0	
15.3884(4)		3 0 0
15.4029(10)	0 2 1	
15.4286(2)		1 0 1
15.4429(2)	1 0 1	

15.4783(4)	4 0 0	
15.4884(5)		4 0 0
15.5094(10)	1 2 1	
15.5274(2)	2 0 1	
15.5422(3)		2 0 1
15.5788(3)	0 0 2	
15.5918(3)		0 0 2
15.6242(4)	3 0 1	
15.6371(4)		3 0 1
15.6750(3)	1 0 2	
15.6897(2)		1 0 2
15.7233(4)	4 0 1	
15.7361(5)		4 0 1
15.7724(3)	2 0 2	
15.7880(3)		2 0 2
15.8208(5)	0 0 3	
15.8348(5)		0 0 3
15.8676(4)	3 0 2	
15.8826(4)		3 0 2
15.9180(3)	1 0 3	
15.9338(4)		1 0 3
15.9647(6)	4 0 2	
15.9805(7)		4 0 2

a. See footnote a in TABLE 3.

TABLE 8

IONIZATION POTENTIALS AND VIBRATIONAL ASSIGNMENTS OF THE $\tilde{A}\ ^2\Pi_u$ PHOTOELECTRON BAND OF CS_2^+.

IP (eV)	Vibrational assignment	
	$\Omega = 3/2$	$\Omega = 1/2$
12.6986(1)[a]	0 0 0	
12.7200(1)		0 0 0
12.7712(1)	1 0 0	
12.7923(1)		1 0 0
12.8431(2)	2 0 0	
12.8638(2)		2 0 0
12.9158(2)	3 0 0	
12.9357(2)		3 0 0
12.9876(5)	4 0 0	
13.0080(5)		4 0 0
13.0569(5)	5 0 0	
13.0773(5)		5 0 0
13.1274(7)	6 0 0	
13.1469(7)		6 0 0
13.1994(9)	7 0 0	
13.2187(9)		7 0 0

13.3381(70)	9 0 0	
13.3571(70)		9 0 0

a. See footnote a in TABLE 3.

TABLE 9

IONIZATION POTENTIALS AND VIBRATIONAL ASSIGNMENTS OF THE $\tilde{B}\ ^2\Sigma_u^+$ AND $\tilde{C}\ ^2\Sigma_g^+$ PHOTOELECTRON BANDS OF CO_2^+.

	IP (eV)	Vibrational assignment
$\tilde{B}\ ^2\Sigma_u^+$	18.0771(1)[a]	0 0 0
	18.1461(5)	0 1 0
	18.2173(6)	0 2 0
	18.2351(1)	1 0 0
	18.3051(6)	1 1 0
		0 0 1
	18.3322(6)	0 4 0
	18.3860(10)	0 1 1
		1 2 0
	18.3941(4)	2 0 0
	18.4594(4)	2 1 0
		1 0 1
	18.5120(30)	1 4 0
	18.5337(3)	0 0 2
		2 2 0
		3 0 0
	18.6120(50)	0 1 2
	18.6430(60)	2 0 1
	18.6544(10)	2 4 0
		0 2 2

	18.6872(50)	4 0 0
$\tilde{C}\ ^2\Sigma_g^+$	19.3944(1)	0 0 0
	19.4705(3)	0 1 0
	19.5432(4)	0 2 0
	19.5660(3)	1 0 0
	19.7568(4)	1 0 1
	19.9268(16)	2 0 1

a. See footnote a in TABLE 3.

TABLE 10

IONIZATION POTENTIALS AND VIBRATIONAL ASSIGNMENTS OF THE $\tilde{B}\ ^2\Sigma^+$ AND $\tilde{C}\ ^2\Sigma^+$ PHOTOELECTRON BANDS OF COS^+.

	IP (eV)	Vibrational assignment
$\tilde{B}\ ^2\Sigma^+$	16.0421(1)[a]	0 0 0
	16.1059(2)	0 1 0
	16.1341(5)	1 0 0
	16.2025(6)	1 1 0
	16.2714(6)	0 0 1
	16.3590(7)	1 0 1
$\tilde{C}\ ^2\Sigma^+$	17.9574(1)	0 0 0
	18.0137(2)	0 1 0
	18.0722(10)	1 0 0
	18.2303(1)	0 0 1
	18.3427(2)	1 0 1
	18.4993(1)	0 0 2
	18.7659(15)	0 0 3

a. See footnote in TABLE 3.

TABLE 11

IONIZATION POTENTIALS AND VIBRATIONAL ASSIGNMENTS OF THE $\tilde{B}\ ^2\Sigma_u^+$ AND $\tilde{C}\ ^2\Sigma_g^+$ PHOTOELECTRON BANDS OF CS_2^+.

	IP (eV)	Vibrational assignment
$\tilde{B}\ ^2\Sigma_u^+$	14.4773(1)[a]	0 0 0
	14.5208(4)	0 1 0
	14.5558(1)	1 0 0
	14.5940(50)	1 1 0
	14.6353(10)	2 0 0
	14.7203(20)	3 0 0
	14.8047(10)	0 0 2
$\tilde{C}\ ^2\Sigma_g^+$	16.1901(1)	0 0 0
	16.2332(8)	0 1 0
	16.2715(2)	1 0 0
	16.3568(6)	2 0 0
	16.3984(5)	0 0 1
	16.4390(30)	3 0 0

a. See footnote a in TABLE 3.

FIGURE CAPTIONS

Fig. 1. Schematic top view of the apparatus: (1) beam source, (2) beam catcher, (3) pass energy selector lens, (4) field lens, (5) kinetic energy scan lens, (6) deflectors, (7) 90° spherical sector pre-analyzer, (8) condutance barrier, (9) 8:1 decelerator lens, (10) hemispherical analyzer, (11) multichannel detector, (12) ion extraction lenses, (13) quadrupole mass filter, (14) differential pumping. The photon sources are located above the plane of the drawing. Not shown are two layers of mumetal surrounding the electron flight path. (After Pollard et al. Ref. 22).

Fig. 2. HeI photoelectron spectra of CO_2^+, COS^+ and CS_2^+ using supersonic molecular beams. The spectra are plotted to the full scale of the $\tilde{X}$ bands. The full scale of the most prominent peak is indicated in each spectrum.

Fig. 3. The $\tilde{X}$ bands of the HeI photoelectron spectra of CO_2^+, COS^+ and CS_2^+. The vibrational assignments of the two spin-orbit split components are indicated. H.B. stands for hot band transition.

Fig. 4. The $\tilde{A}$ bands of the HeI photoelectron spectra of CO_2^+, COS^+ and CS_2^+. The vibrational assignments of the two spin-orbit split components are indicated. In CO_2^+ and COS^+, the $\tilde{A}$ bands overlap with the $\tilde{B}$ bands, which are indicated in the figures. H.B. stands for hot band transition. β stands for the HeI β line spectrum.

Fig. 5. The $\tilde{B}$ bands of the HeI photoelectron spectra of CO_2^+, COS^+ and

CS_2^+, with the vibrational assignments. In CO_2^+ and COS^+, assignments for the components from the $\tilde{A}$ bands are not indicated.

Fig. 6. The $\tilde{C}$ bands of the HeI photoelectron spectra of CO_2^+, COS^+ and CS_2^+ with the vibrational assignments.

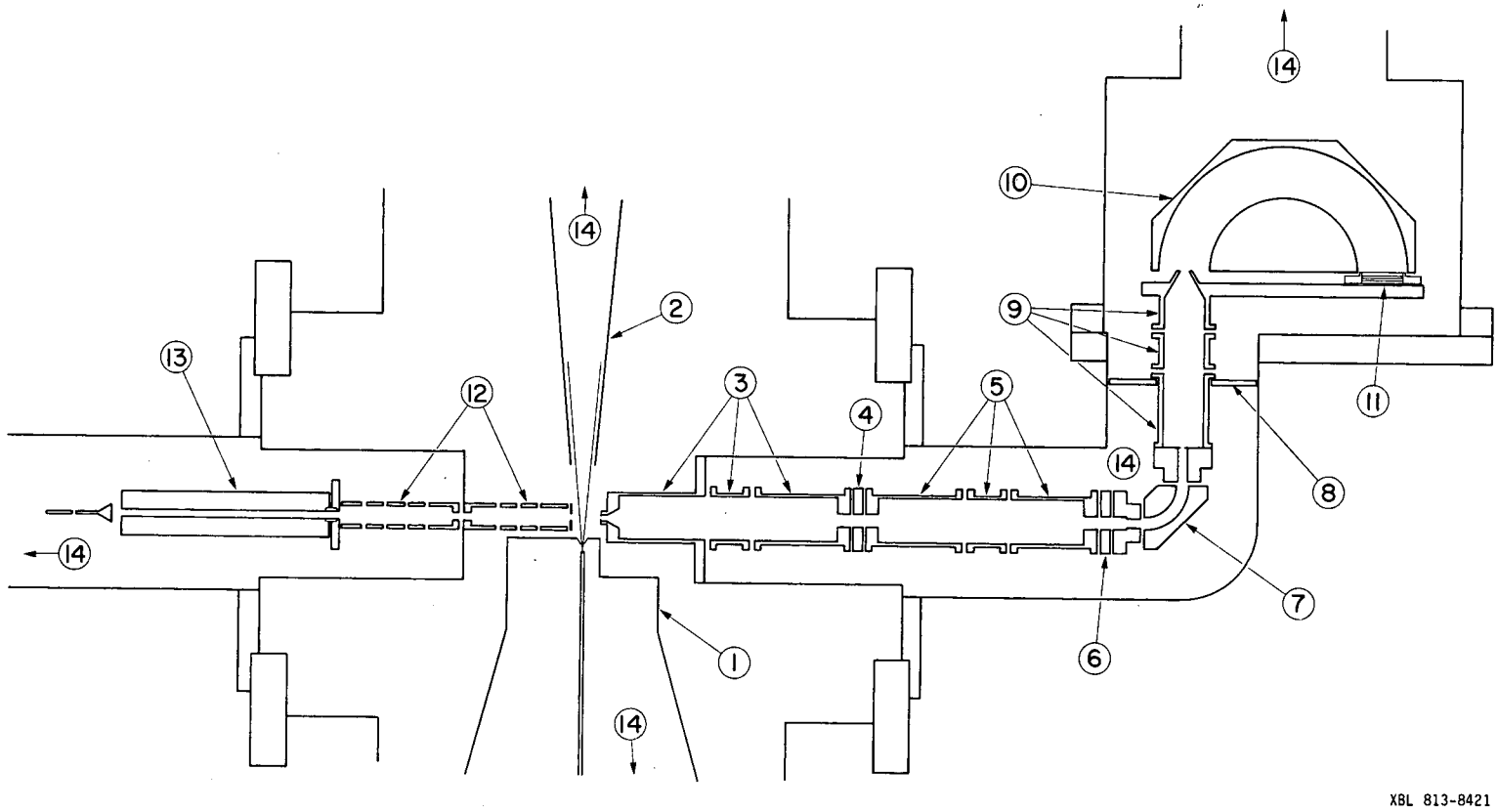

Figure 1

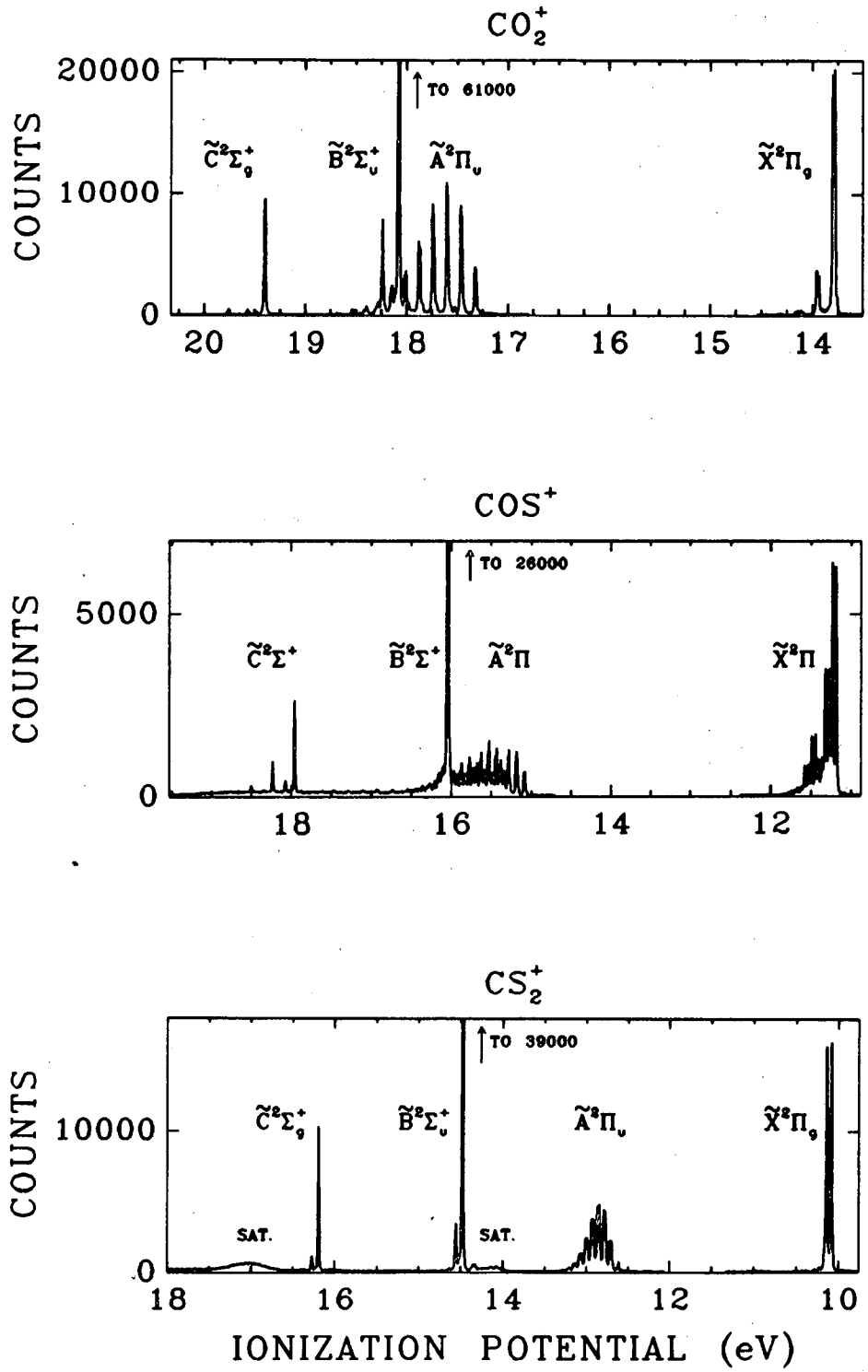

XBL 878-3608

Figure 2

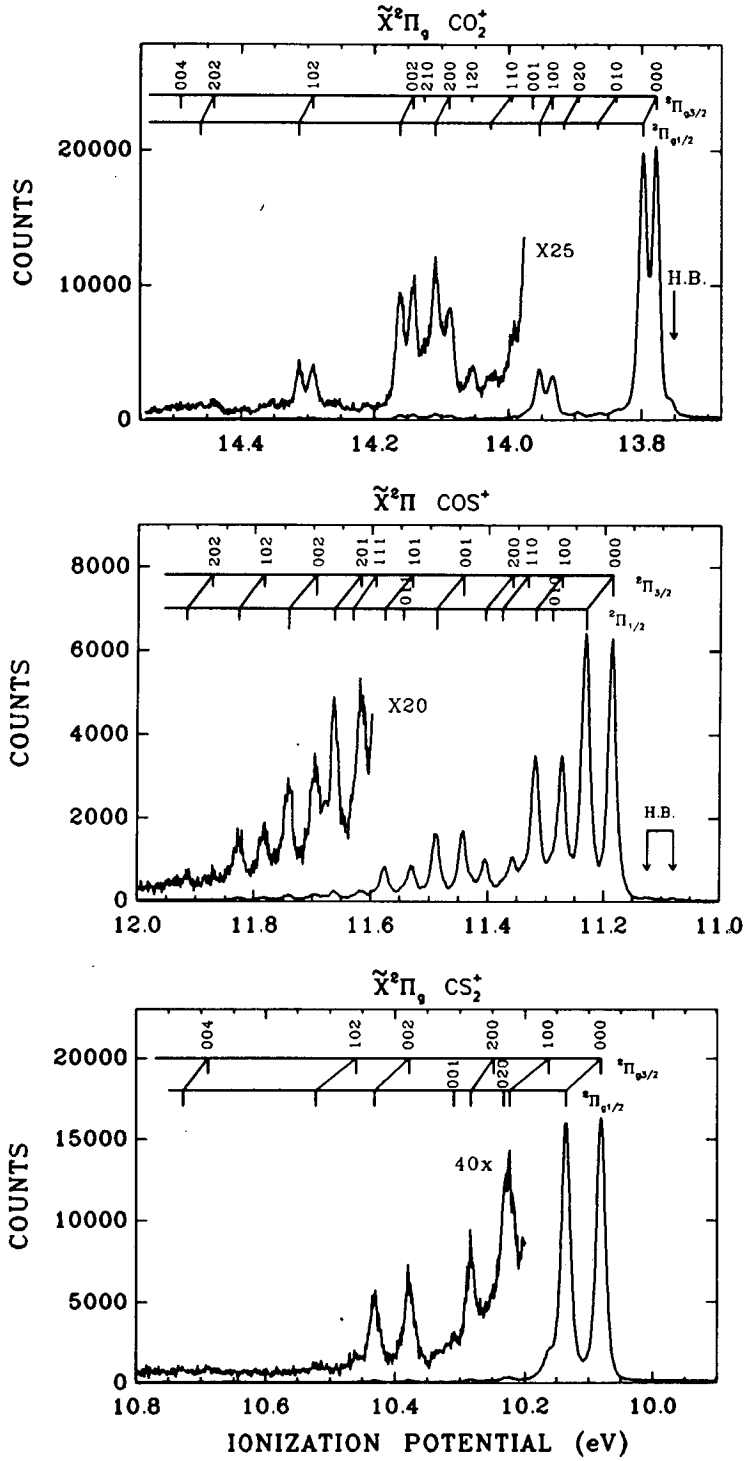

XBL 878-3609

Figure 3

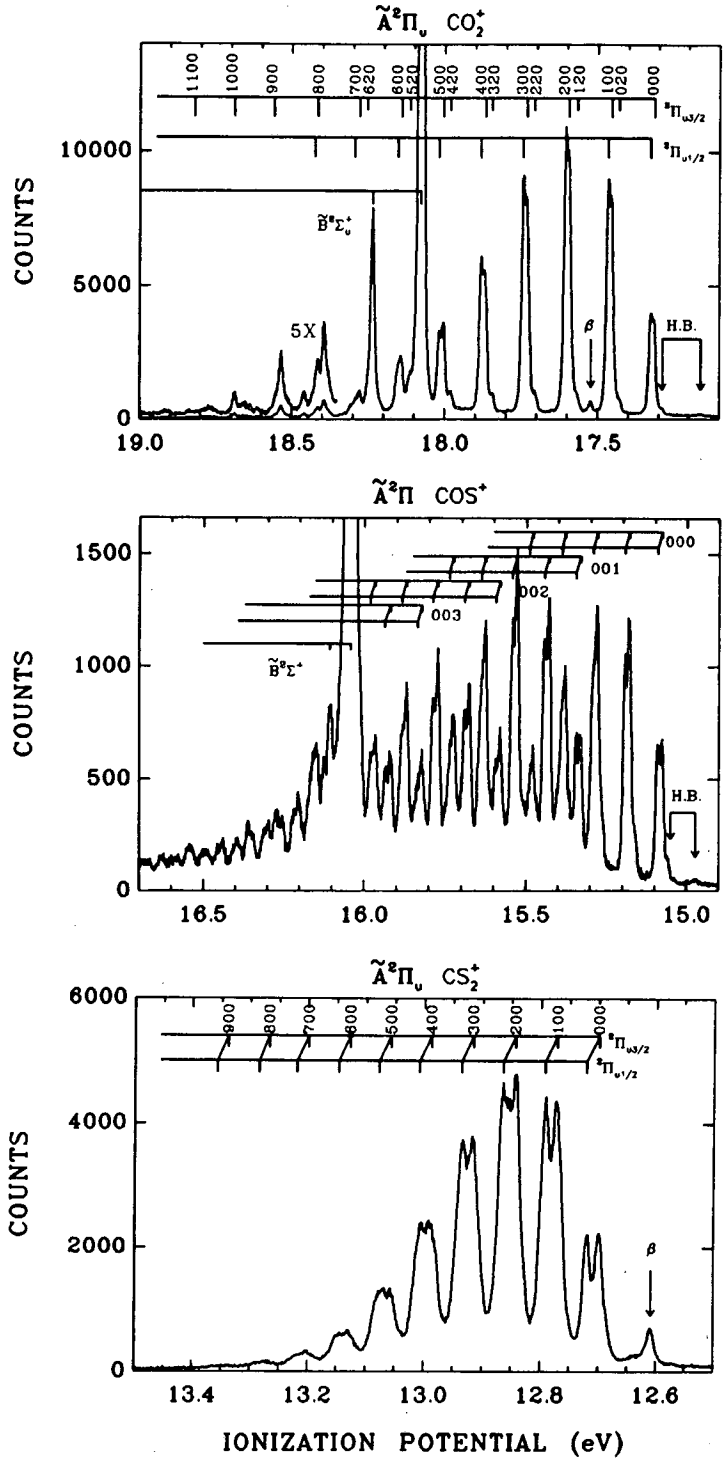

XBL 878-3610

Figure 4

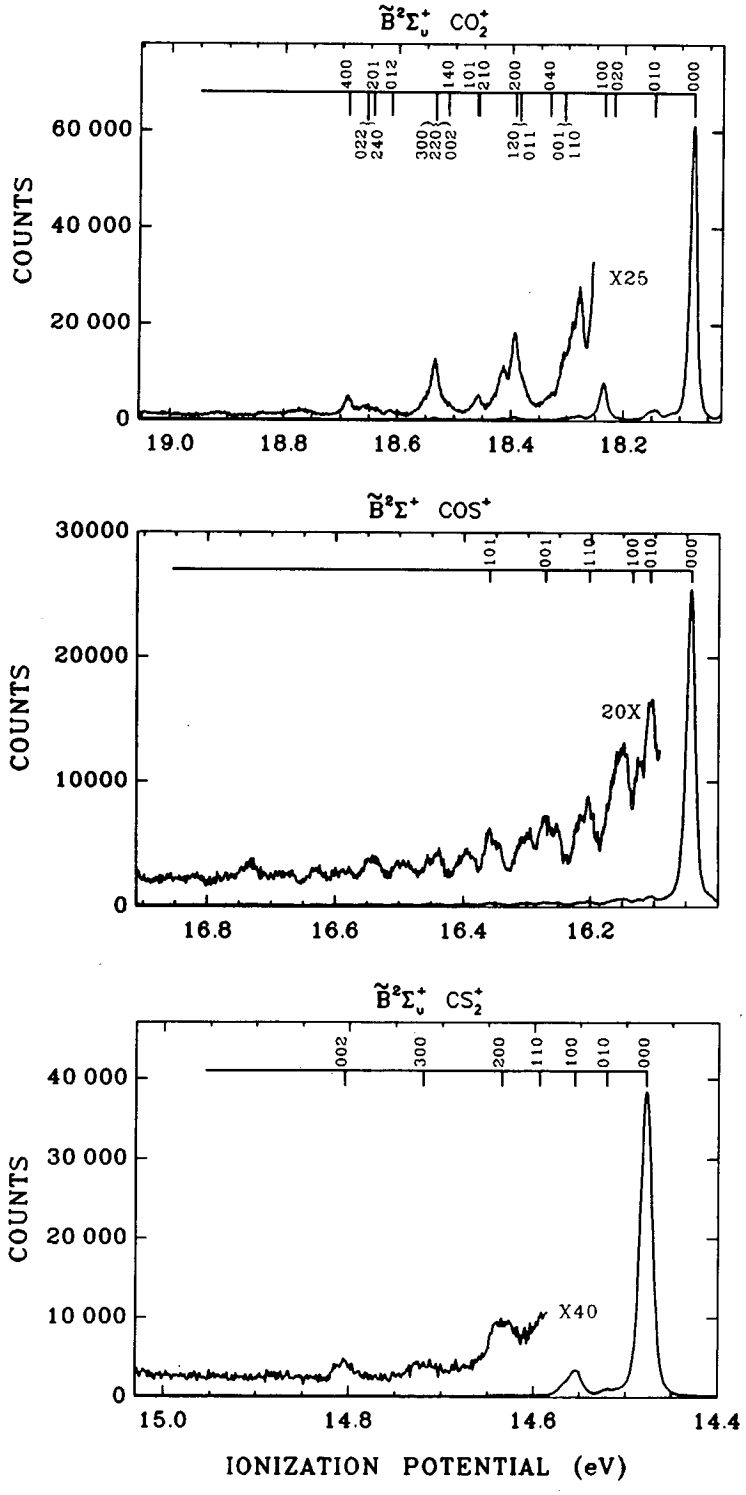
$\tilde{B}^2\Sigma_u^+$ CO_2^+
COUNTS
60 000
40 000
20 000
0
X25
19.0
18.8
18.6
18.4
18.2
$\tilde{B}^2\Sigma^+$ COS^+
30000
20000
10000
20X
16.8
16.6
16.4
16.2
$\tilde{B}^2\Sigma_u^+$ CS_2^+
40 000
30 000
20 000
10 000
X40
15.0
14.8
14.6
14.4
IONIZATION POTENTIAL (eV)
XBL 878-3611

Figure 5

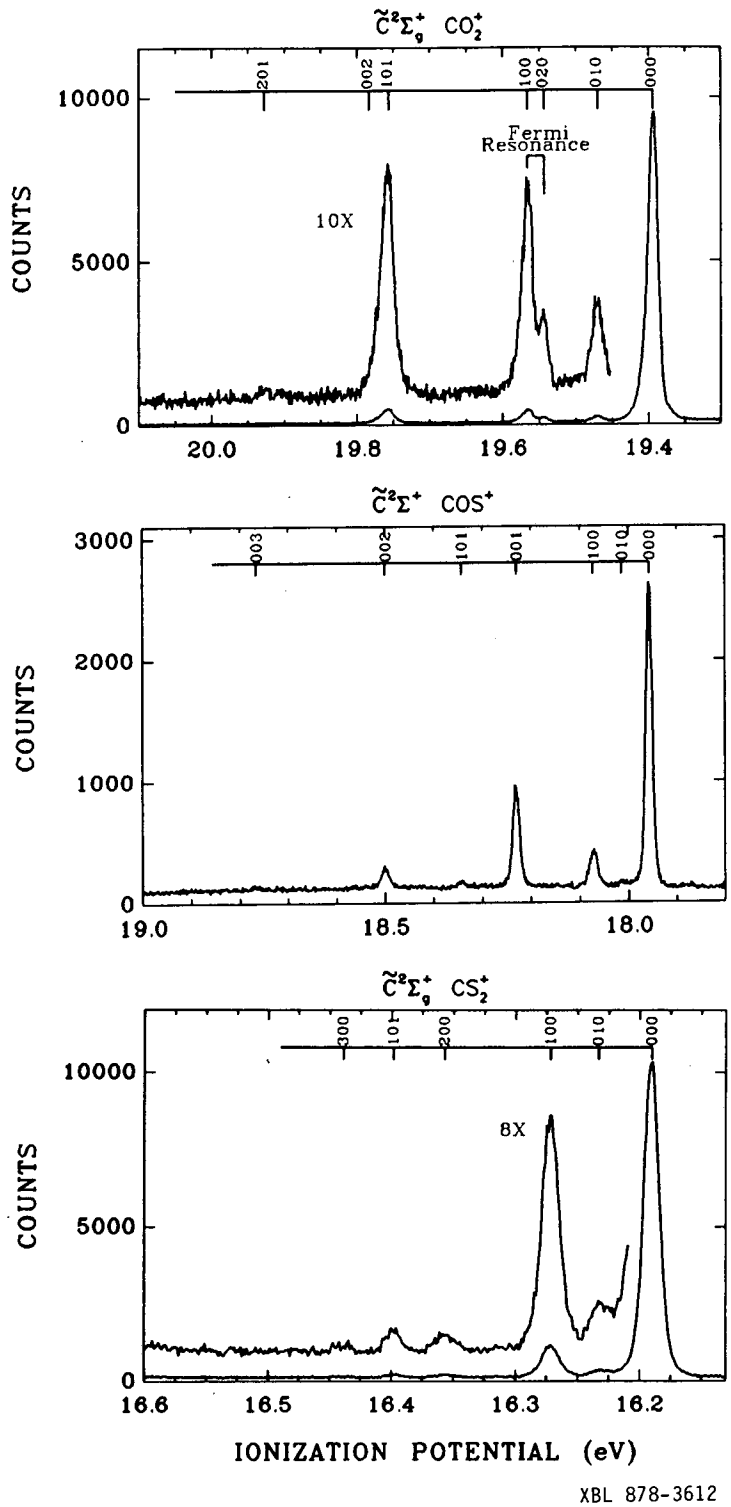

XBL 878-3612

Figure 6

LAWRENCE BERKELEY LABORATORY
TECHNICAL INFORMATION DEPARTMENT
UNIVERSITY OF CALIFORNIA
BERKELEY, CALIFORNIA 94720